KSCE Journal of Civil Engineering (2017) 21(3):937-949
DOI 10.1007/s12205-016-0871-0

Structural Engineering
pISSN 1226-7988, eISSN 1976-3808
www.springer.com/12205

A Comparative Study of Live Load Distribution in Skewed Integral and Simply Supported Bridges

O. Fatih Yalcin*

Received October 16, 2015/Accepted April 26, 2016/Published Online July 7. 2016

Abstract

In this study, the effects of skew and superstructure-abutment continuity on the distribution of live load effects among the girders of Skewed Integral Abutment Bridges (SIBs) and Skewed Simply Supported Bridges (SSBs) is investigated comparatively. For this purpose, numerous 3-D and corresponding 2-D finite element models of several single span SIBs and SSBs are built. Analyses of the models are then conducted under AASHTO live load. In the analyses, the effect of various skew angles and superstructure properties such as girder size and spacing, number of girders, span length as well as slab thickness are considered. The results from the analyses are then used to calculate the Live Load Distribution Factors (LLDFs) for the girders of SIBs and SSBs as a function of skew and the above-mentioned structural parameters. LLDFs and Skew Correction Factors (SCFs) are also obtained from AASHTO equations developed for SSBs. These LLDFs and SCFs are compared with those calculated from the analyses in order to assess the applicability of AASHTO equations to SIBs. The results revealed that live load distribution of moment and shear among the girders is improved in SIBs compared to SSBs. Increase in skew generally decreases the live load effects among the girders of SIBs.

Keywords: *integral bridge, jointed bridge, skew, continuity, live load*

1. Introduction

Integral bridges (IBs) have no expansion joints. They possess a structural system mainly consists of stub abutments supported on a single row of steel H-piles. In these type of bridges, the abutments are cast integral with the deck and the girders. The monolithic construction of the slab and girders with abutments in IBs provide torsional and rotational rigidity to the slab and the girders. Consequently, under live loads, the superstructure and abutments act together because of the continuity at the superstructure – abutment joint. IBs have many economical and functional advantages over regular jointed bridges. Therefore, straight and skewed IBs (SIBs) are becoming more and more popular in North America and Europe (Burke, 2009; Franchin and Pinto, 2014; David *et al*., 2014; Feldmann *et al.*, 2011).

Skewed IBs are common in highways to accommodate geometry constraints due to space limitations. SIBs are characterized by the acute angle (θ) between the abutment and the normal to the centerline of the bridge deck as shown in Fig. 1(a). Many practicing engineers use simplified two-dimensional structural models together with Live Load Distribution Factors (LLDFs) and skew correction factors to estimate live load effects in the girder for design purposes. However, these factors were developed solely for SSBs. Although construction of straight IBs and SIBs are very common, Live Load Distribution Factors (LLDFs) for IBs and Skew Correction Factors (SCFs) for SIBs have not been implemented in design codes yet. Hence, many design engineers neglect the superstructure- abutment continuity and use provisions for LLDFs for jointed bridges in current bridge design specifications such as AASHTO LRFD (2014) to design IBs. Although numerous studies (Zokaie, 2000; Khaloo and Mirzabozorg,2003; Ebeido and Kennedy, 1996; Nouri and Ahmadi, 2011) are conducted on live load effects in SSBs, similar works for IBs and SIBs are very rare. Dicleli and Erhan (2009) and Erhan and Dicleli (2009) have found that AASHTO LRFD formulas for live load distribution factors are not suitable for estimating the live load effects for IB components. Consequently, new equations of LLDFs for IBs were proposed in these studies. However, similar research on the applicability of Skew Correction Factors (SCFs) developed for regular jointed bridges to SIBs is not present in the literature. Only recently, some parametric studies (Dicleli and Yalcin, 2014; Yalcin, 2015) were conducted to investigate various truck loading patterns and positions to attain maximum live load effects in components of SIBs.

Accordingly, in this research a comparative study is conducted to investigate the effect of skew and the effect of superstructure-abutment continuity on the distribution of live load effects among the girders of SIBs. To the author's best knowledge, this paper is the first one that addresses the effect of superstructure – abutment continuity on live load distribution among the girders of SIBs. Thus, the study will potentially be very important to

*Assistant Professor, Dept. of Civil Engineering, Istanbul University, Avcilar, Istanbul, Turkey (Corresponding Author, E-mail: fyalcin@gmail.com)

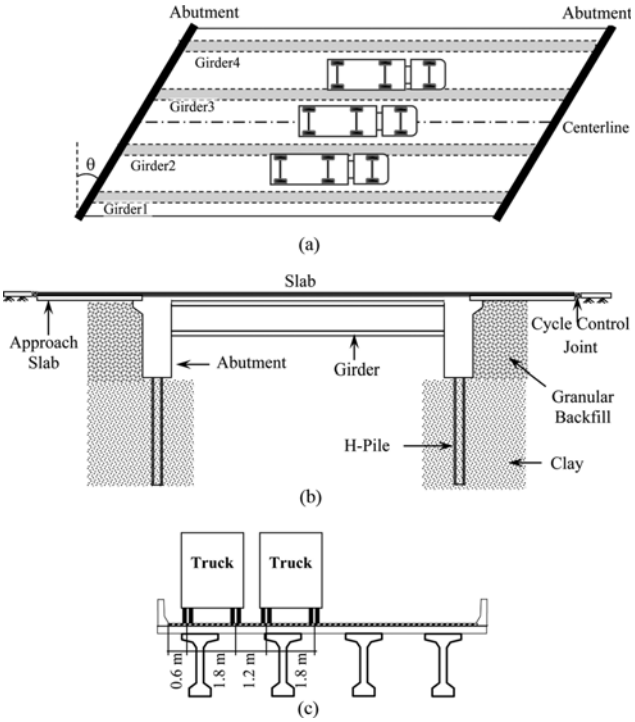

Fig. 1. (a) Plan View of a Typical Single Span SIB under Truck Loading, (b) Elevation View of the SIB, (c) Typical Slab-on-girder Bridge Cross-section and Minimum Clearances Under Truck Loading

open the way for further research in this specific area. In order to make the comparisons, numerous SSB and SIB finite element models having the same superstructure properties are analyzed under the same live load cases to obtain LLDFs for girder shear and moment. Then, these LLDFs for SSBs and SIBs are compared with those obtained from AASHTO LLDF equations. The results from this research study will help to understand the behavior of SIBs under live loads and to assess the applicability of AASHTO procedures, which are solely developed for SSBs, to the design of SIBs.

2. Scope and Assumptions

The research study is focused on slab-on girder SSBs and SIBs with single span. The bridges are assumed to have AASHTO type prestressed concrete girders which are commonly used in bridge construction. The elevation and cross-section of a typical SIB are shown in Fig. 1(b) and (c), respectively. The cross-section of SSBs is also similar to that shown in Fig. 1(c). The abutment of SIBs are assumed as supported by steel H-piles. A moment connection is assumed between the piles and the abutment as well as between the superstructure and the abutment per current state of design practice. Granular material commonly used in construction of IBs is assumed for the backfill behind the abutments while cohesive soil (clay) is assumed for the pile foundations (Fig. 1(b)).

3. Bridge Parameters

To investigate the effect of skew and the effect of superstructure-abutment continuity on the live load distribution among the girders of SIBs, comparative live load analyses of both SSBs and SIBs with various bridge parameters are conducted. The diaphragms at the supports of SSBs are assumed to have a rectangular cross-section with a width of 0.4 m. The abutments of the SIBs considered in this study are assumed to be 3 m tall and supported by 12 m long end-bearing steel HP 250 × 85 piles. The number of piles is taken same as the number of girders. The strength of the concrete used for the prestressed concrete girders are assumed to be 50 MPa while those of the slab, diaphragms (for SSBs) and the abutments (for SIBs) are assumed to be 30 MPa. In an earlier research study (Dicleli and Erhan, 2008), the variations in substructure, backfill and foundation soil properties are found to have negligible effects on the distribution of live load moment and shear among the girders of straight IBs. In order to further verify these findings for SIBs, sensitivity analyses are conducted to determine the effect of soil properties on LLDFs. For this purpose, three different values of undrained

Table 1. Parameters Considered in the Analyses

Skew (degree)	L (m)	S (m)	GT	N_b	t_s (m)	C_u (kPa)	γ (kN/m^3)
0;10;20;30; 40;50;60	**15;20;25; 30;35;40**	2.4	IV	4	0.20	40	20
0;10;20;30; 40;50;60	30	**1.2; 2.4; 3.6; 4.8**	IV	4	0.20	40	20
0;10;20;30; 40;50;60	30	2.4	**II;III; IV;V**	4	0.20	40	20
0;10;20;30; 40;50;60	30	2.4	IV	**4; 5; 6; 7**	0.20	40	20
0;10;20;30; 40;50;60	30	2.4	IV	4	**0.15;0.20; 0.25;0.30**	40	20
0;10;20;30; 40;50;60	30	2.4	IV	4	0.20	**20;40;80**	20
0;10;20;30; 40;50;60	30	2.4	IV	4	0.20	40	**18;20;22**

shear strength for foundation soil (C_u = 20, 40, 80 kPa) and unit weights of granular backfill (γ = 18, 20 and 22 kN/m^3) are considered. The results of these preliminary sensitivity analyses revealed that the variations in soil properties change the LLDFs at most by 1.8%. Hence, consistent with the findings of Dicleli and Erhan (2008), the effect of soil properties on LLDFs for girder moment and shear is considered as insignificant. Therefore, in this study the structural parameters considered for comparative purposes are limited to superstructure parameters only. In the analyses, the skew angle is taken as the main parameter. Accordingly, for the SIBs and SSBs considered in this study, the skew angles are assumed to vary between 0° to 60° with 10° increment. The cantilever length measured form the centroid of the external girder up to the face of the barrier wall (d_e) for both SSBs and SIBs is taken as 0.9 m. This property solely affects the live load distribution in exterior girders. Superstructure properties considered in the analyses include span length (L), girder spacing (S) and type (GT), number of girders (N_b) as well as the slab thickness (t_s). The range of values considered for each parameter is given in Table 1. This resulted in 252 different 3-D and corresponding 2-D structural models of SSBs and SIBs and more than 11,000 analyses cases. The 11,000 analyses cases include the analyses of both 2-D and 3-D models, the analyses for various longitudinal positions of the truck to estimate the maximum girder shear and moment and the analyses for various transverse positions of one, two or more trucks in the analyses of 3-D models.

4. Three-Dimensional Structural Model

The 3D structural models of the above-mentioned SSBs and SIBs are built and analyzed by using a finite-element based software (SAP2000, 2014). The 3D structural models of typical SSB and SIB used in the analyses are shown in Figs. 2(a) and 2(b) respectively.

4.1 Superstructure Modeling for SSB and SIBs

A finite element modeling technique similar to that proposed Hays *et al.* (1986), which has already been verified by Yousif and Hindi (2007) and Mabsout *et al.* (1997), is used to model the slab-on-girder deck of SSBs and SIBs used in this study. This superstructure model is chosen specifically because of its simplicity, which provide great ease in automatic generation of the huge number of bridge models. Further details of this model and comparisons with other more complicated models (Imbsen and Nutt, 1978; Brockenbrough, 1986; Tarhini and Frederick, 1992) are summarized and discussed by Erhan and Dicleli (2009). Accordingly, the bridge slab is modeled using quadrilateral shell elements and the girders are modeled using 3-D beam elements as shown in the 3-D structural models presented in Fig. 2. Full composite action between the slab and the girders is assumed in the models by adjusting the moment of inertia of the girder.

For the SIB and SSB models, the slab is modeled using parallelogram quadrilateral shell elements where the sides of the parallelogram shell elements are parallel to the skewed abutments. This type of meshing facilitates the placement of truck wheel loads and automatic generation of the shell elements. The side length in the longitudinal direction and the height of the parallelogram shell elements are taken as 0.6 m.

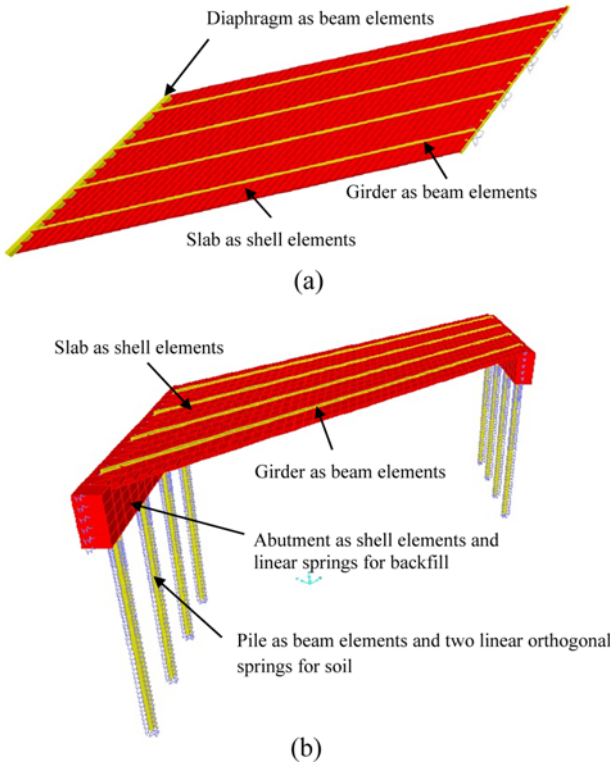

Fig. 2. 3D Structural Model of a Typical: (a) SSB, (b) SIB

4.2 Substructure Modeling of SIBs

In this study, the abutments are modeled using Mindlin shell elements to take into consideration shear deformations and the piles are modeled using 3-D beam elements. The abutment is divided into rectangular shell elements with a transverse dimension of 0.6 m for the purpose of being compatible with the superstructure shell dimension. Sensitivity analyses conducted on the models show that the current mesh sizes are adequate as the analyses results do not differ for smaller mesh size. Further details about these modeling techniques can be found in Dicleli and Erhan (2008).

4.3 Modeling of Soil-structure Interaction Effects for SIBs

For modeling the soil-structure interaction effects in SIBs, a linear elastic behavior is assumed due to the small lateral displacements of the abutments and piles under live load effects. To model the interaction effects between backfill and abutment, a set of linear springs are connected at the interface nodes on the abutment as illustrated in Fig. 2(b). Similarly, for soil-pile interaction effects horizontal linear springs in orthogonal directions are attached at each node along the pile. The stiffness calculations and spacing of these linear springs for medium-stiff clay and

more detailed description of the soil-structure interaction modeling for IBs can be found in Dicleli and Erhan (2008).

5. Two-Dimensional Structural Model

In order to calculate LLDFs, 2-D frame version for each 3-D structural model of the SSBs and SIBs is also built. These models are built using 2-D elastic beam elements considering a single girder. In the structural models, the tributary width of the slab and abutment is set equal to the spacing of the girders. The soil-structure interaction modeling for the 2-D model of SIBs is similar to that for the 3-D model except the spring constants are calculated using a tributary area equal to the girder spacing times the vertical spacing between the nodes.

6. Live Load Model and Estimation of LLDFs

The FEAs are performed using the AASHTO LRFD design live load designated as HL-93. HL-93 includes a design truck or a tandem and a lane load. Since the design lane load was not considered in the development of the live load distribution factors in AASHTO LRFD, the analyses are performed using the design truck alone. For the cases where multiple design lanes are loaded, the AASHTO LRFD spacing limitations used in the analyses for the transversely positioned trucks are shown in Fig. 1(c).

The maximum load effect on a bridge is based on the position of the truck both in the longitudinal and transverse directions, the number of trucks in the transverse direction (i.e. the number of loaded design lanes) together with the probability of the presence of multiple loaded design lanes. First, the design truck longitudinal position is obtained by influence line analyses. Then, the design trucks are moved transversely along the bridge width to obtain the maximum live load effects. This procedure is repeated for the estimation of critical truck transverse positions for the maximum girder moment (M_g) and shear (V_g) in both SSBs and SIBs due to live load.

For non-skewed bridges, the adjacent trucks are positioned at equal distances from the abutment, and therefore the truck loading position along the length of the bridge in a 3-D model completely coincides with that of the 2-D frame model. However, in the case of SIBs various longitudinal positions can be used to place trucks on each lane of 3-D model for the same 2-D model, which results in different loading patterns. In recent studies (Dicleli and Yalcin, 2014; Yalcin, 2015), some predetermined loading patterns and all possible truck loading configurations are investigated to determine the most critical loading pattern producing the maximum live load effects in SIB components. The results in these studies revealed that trucks, which are placed diagonally across the width of the bridge (diagonal loading pattern), are observed to produce the most unfavorable live load effects in bridge components. Hence, in this study, the centerline of axle loads of multiple adjacent trucks are applied to the bridge deck at equal distances from the skewed abutment as shown in Fig. 1(a).

LLDFs are calculated for the composite interior and exterior girders of SSBs and SIBs considering the loading cases where only a single design lane is loaded and two or more design lanes are loaded. For the composite interior girders, the maximum live load effects (moment and shear) from 3-D analyses are calculated as the summation of the maximum effects in the girder element and within the tributary width of the deck at the same location along the bridge. The LLDFs are then calculated as the ratio of the maximum live load effects obtained from 3-D analyses to those obtained from 2-D analyses under a single truck loading.

7. Parametric Studies and Analyses Results

In the case of skewed bridges, the skewed supports change the load path exerted by live load. The live load exerted on the bridge deck is transferred to the supports in their shortest path, which is the path extending toward the obtuse corners. Consequently, when compared to LLDFs of non-skewed IBs with similar properties (same span length, number of girders, slab thickness, girder size and spacing), the LLDFs for SIB girders are greatly depend on the skew angle. Accordingly, in this section the effect of skew angle is discussed together with various superstructure parameters.

Due to the nature of the study, a large number of loading cases and SIB models with various skews are required. This necessitates an automated procedure. For this purpose, a Visual Basic for Applications (VBA) program is coded within Excel to employ the Open Application Programming Interface (OAPI) of SAP2000 to create, modify and run models, then to write the results into the spreadsheet for further processing. The OAPI makes possible the tedious and time-consuming processes of generating bridges having various skews from a master bridge model, creating load cases, applying wheel loads for each load case and extracting the results.

The VBA program and Excel spreadsheets are used together to prepare the FEMs of SIBs in the FEA software and to extract the results from the output files generated by the FEA software. The program requires as input data: the length, width, height and skew of the bridge, and the properties used for applying the truck loads in the FEMs. Using these input parameters, the program prepares the FEMs having 0°, 10°, 20°, 30°, 40°, 50°, and 60° skew angles; creates the load cases and calculates the wheel loads that change when the geometric properties of the bridge changes. FEA software requires the wheel loads to be assigned to the shell nodes only. However, the calculated wheel positions may not coincide with the exact positions of the shell nodes. Therefore, in such cases, an inverse ratio procedure is used to distribute the wheel loads to the shell nodes. This procedure is carried out for each loading point, which does not coincide with the existing shell nodes. For the SIB models considered in the analyses, the wheel loads are distributed to the shell nodes as described above for all of the load cases.

The maximum live load effects are obtained from 3-D analyses

by using the Section Cut command of the FEA software. The resultant of live load effects in the girder and within the tributary area of the slab is calculated by defining section cuts along the girder. In order to precisely determine the maximum live load effects, numerous adjacent section cuts are defined with a spacing of 0.2 m along each girder. Then, the maximum live load moment and shear for both internal and external girders from the resultants of section cuts is found by the aforementioned VBA program.

The parametric analyses results are presented in the following sections. In the relevant figures (Figs. 3-7), the analyses results for the interior girder moment and shear for the case where only one design lane loaded are designated by **IntM1** and **IntV1** respectively, while those for the case where two or more design lanes loaded are designated by **IntM2** and **IntV2**. Similar designations for the exterior girder moments are also used as; **ExtM1**, **ExtV1**, **ExtM2** and **ExtV2** where, "Int and "Ext stand for interior and exterior girders respectively, M and V stand for girder moment and shear respectively and finally 1 and 2 stand for one design lane loaded and two or more design lanes loaded cases respectively.

In the relevant figures, the LLDFs obtained for the interior and exterior girders of SIBs, SSBs and those calculated from AASHTO LRFD are compared. The comparisons are made for loading cases where only one design lane is loaded and two or more design lanes are loaded. Furthermore, as the skew increases from 0° to 60°, percentage increase values in LLDFs for all live load effect of SSBs, SIBs and AASHTO are presented in Tables 3-7. In the comparisons, as the skew changes, the variation of LLDFs of SIBs and the effects of superstructure – abutment continuity on LLDFs are examined.

7.1 AASHTO LLDF and Skew Correction Factor (SCF) Equations

The AASHTO LLDF and skew correction factor equations for the composite girder moments and shears of slab-on-girder jointed bridges (SSBs) for the cases where one design lane is loaded and two or more lanes are loaded are given in Table 2. In the table K_g is a parameter representing the longitudinal stiffness of the composite slab-on girder section of the bridge, which is related to the girder properties. It can be deduced from the table that skew tends to decrease the girder moments and increase the girder shears. It should be noted that the skew tends to increase the shear LLDFs only for the exterior beam at the obtuse corner. However, in order to be on the conservative side, in AASHTO it is stated that SCF for the exterior girder in the obtuse corner

Table 2. AAHSTO LRFD LLDF and Skew Correction Factor Equations

	Interior Girder	Exterior Girder	Skew Corr. Factor
Moment One Lane	$0.06+\left(\frac{S}{4300}\right)^{0.4}\left(\frac{S}{L}\right)^{0.3}\left(\frac{K_g}{Lt_s^3}\right)^{0.1}$	Lever Rule	$1-c_1(\tan\theta)^{1.5}$ $c_1=0.25\left(\frac{K_g}{Lt_s^3}\right)^{0.25}\left(\frac{S}{L}\right)^{0.5}$ if $\theta<30^o$ then $c_1=0.0$ if $\theta<60^o$ use $\theta=60^o$
Moment Two Lane	$0.075+\left(\frac{S}{2900}\right)^{0.6}\left(\frac{S}{L}\right)^{0.2}\left(\frac{K_g}{Lt_s^3}\right)^{0.1}$	$g=e\,g_{interior}$ $e=0.77+\frac{d_e}{2800}$	
Shear One Lane	$0.36+\frac{S}{7600}$	Lever Rule	$1.0+0.20\left(\frac{Lt_s^3}{K_g}\right)^{0.3}\tan\theta$
Shear Two Lane	$0.2+\frac{S}{3600}-\left(\frac{S}{10700}\right)^{0.2}$	$g=e\,g_{interior}$ $e=0.6+\frac{d_e}{3000}$	

Table 3. The Percentage Increase in LLDFs foR Various Span Lengths

		IntM1	IntM2	ExtM1	ExtM2	IntV1	IntV2	ExtV1	ExtV2
SSB	L=15	-12.1	-21.8	-9.1	-8.3	-3.5	-22.5	0.0	0.0
	L=20	-13.1	-19.7	-9.1	-8.7	2.1	-17.6	3.4	3.3
	L=30	-10.3	-14.6	-9.6	-9.8	6.0	-12.0	6.9	7.0
	L=40	-7.0	-12.5	-9.8	-9.6	9.4	-7.7	8.8	8.7
SIB	L=15	-6.4	-18.5	-0.1	-12.5	-15.2	-22.4	-11.2	-9.1
	L=20	-8.2	-16.8	-0.4	-9.0	-13.0	-21.4	-11.1	-9.1
	L=30	-9.2	-15.8	-1.9	-5.5	-10.8	-19.8	-10.7	-8.7
	L=40	-7.9	-13.9	-2.5	-4.8	-9.8	-18.1	-10.2	-8.7
AASHTO	L=15	-34.2				21.3			
	L=20	-27.6				23.2			
	L=30	-20.3				26.2			
	L=40	-16.4				28.6			

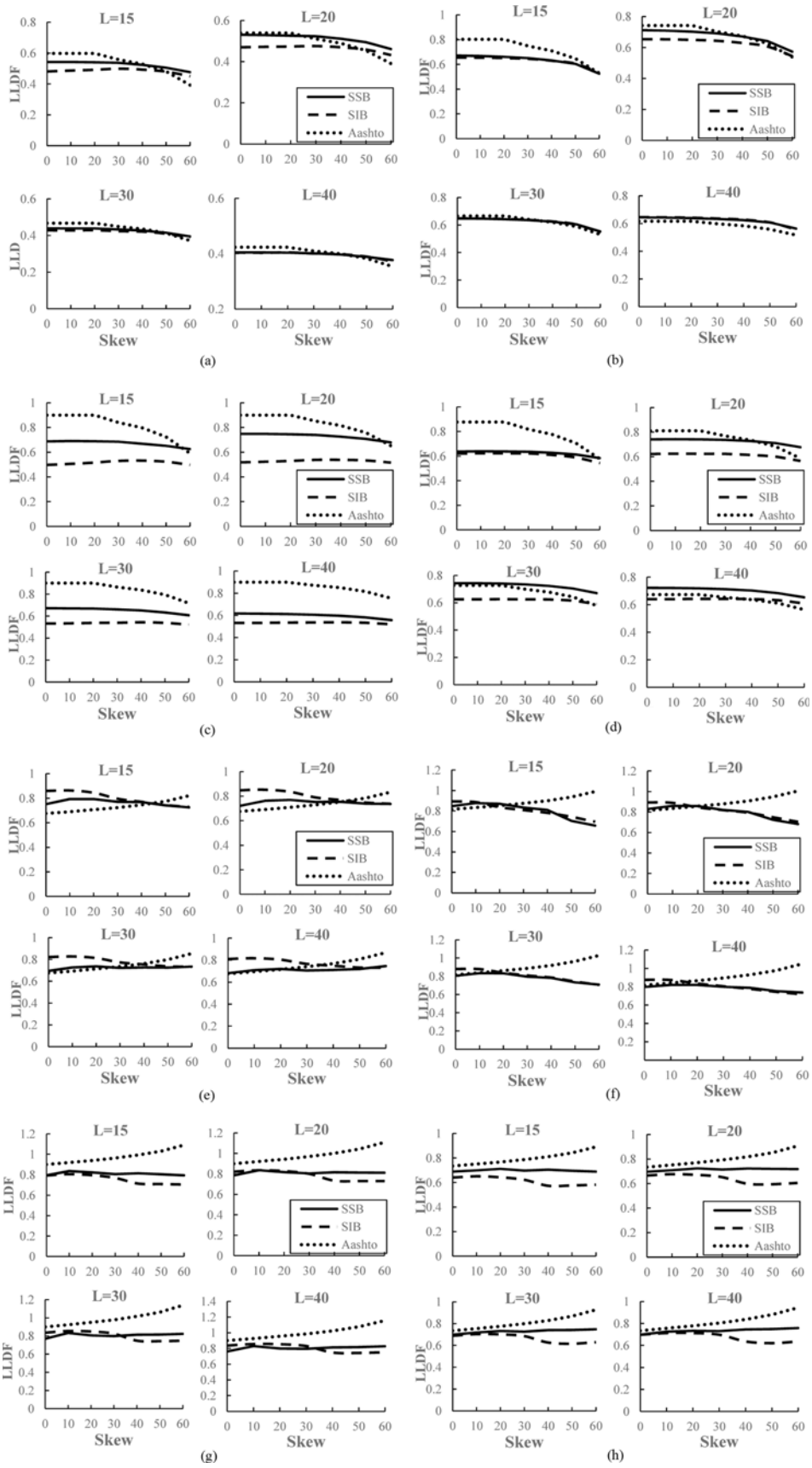

Fig. 3. Moment and Shear LLDFs vs. Skew Angles for Span Lengths (L) of 15 m, 20 m, 30 m, and 40 m: (a) IntM1, (b) IntM2, (c) ExtM1, (d) ExtM2, (e) IntV1, (f) IntV2, (g) ExtV1, (h) ExtV2

should be applied to all girders in a multibeam bridge.

7.2 Effect of Skew and Continuity Versus Span Length

The effects of skew and continuity on the distribution of girder live load moment and shear are illustrated in Fig. 3 for span lengths of 15, 20, 30, 40 m. In the figures, the LLDFs obtained for SSBs, SIBs and those calculated from the AASHTO formulae for the interior and exterior girders of slab-on-girder bridges are compared. In order to provide the reader with a better interpretation of the results, in Table 3, the percentage increases in the LLDFs for interior and exterior girder moment and shear are given for various span lengths (L). The percentage increases are calculated as the difference between the LLDFs of the straight and 60° skewed bridges divided by the LLDFs of the straight bridges. Negative values indicate a decrease in the girder LLDF with increasing skew angle. It should also be noted that, the values in the table actually correspond to 100* (SCF–1) for 60° skew angle.

From Figs. 3(a)-(d) it is observed that, as the skew angle increases, LLDFs for exterior girder moment for the case where one lane is loaded (ExtM1) decreases for SSBs and AASHTO while it remains almost constant for SIBs regardless of the span length. However, for the cases of IntM1, IntM2 and ExtM2 cases skew tends to decrease the LLDF for both bridge types and AASHTO. AASHTO produces reasonable estimates of LLDF for interior girder moments especially for longer span lengths. This may be attributed to the fact that, in longer span bridges, the distribution of girder moment improves as the supports get further away from the truck loading position, and the effect of continuity on the LLDFs in SIBs become less noticeable. From Table 3 it is observed that, the decreasing effect of skew on LLDF is less pronounced for SIBs due to superstructure-abutment continuity. It is also observed from the table that for short span bridges, the effect of skew on LLDFs for interior girder moment is more significant than those for exterior girder moment.

For the girder shear, while the skew increases, an increase in LLDFs is observed (see Table 3) for SSBs except for the case of IntV2. This increase is more pronounced for larger span lengths. However, for the case of IntV2 a significant decrease comes out especially for shorter span bridges. Contrary to that, as mentioned previously, AASHTO specifies an increase in shear LLDFs for all the girders in a multibeam bridge with increasing skew. The effect of superstructure-abutment continuity in SIBs produces an important change in the variation of LLDFs as a function of the skew angle (see Figs. 3(e)-(h) and Table 3). For SIBs, shear LLDFs for all types of girder and load cases decreases as the skew increases. This is completely opposite to AASHTO predictions. The effect of span length on SCFs (or percentage increase) for shear in SIBs is less pronounced compared to that in SIBs.

In view of the discussions above, it may be concluded that superstructure – abutment continuity has a significant effect on the LLDFs for both girder shear and moment with respect to the magnitude of the skew angle. Therefore, new SCFs for LLDFs of SIBs should be defined. Furthermore, Fig. 3 and Table 3 reveal that, variation of LLDFs for different live load effects has some complicated sensitivity to the span length. For instance, ExtV1 and ExtV2 are insensitive to the change in span length; however, LLDFs for the other internal forces are sensitive to some extent. Consequently, span length should be considered as a parameter for the development of SCFs for SIBs.

7.3 Effect of Skew and Continuity versus Girder Type

The effects of skew and continuity on the distribution of girder live load moment and shear are illustrated in Fig. 4 for girder types of 2, 3, 4 and 5. In the figures, the LLDFs obtained for SSBs, SIBs and those calculated from the AASHTO formulae for the interior and exterior girders of slab-on-girder bridges are compared. Additionally, in Table 4 the percentage increases in the LLDFs, as the skew angle is increased from 0° to 60°, are given for interior and exterior girder moment and shear for various girder types (GT).

For the girder moment, Figs. 4(a)-(d) and Table 4 reveal that, skew decreases the LLDFs for both types of bridges. This effect is more pronounced for interior girders. As the girder size

Table 4. The Percentage Increase in LLDFs for Various Girder Types

		IntM1	IntM2	ExtM1	ExtM2	IntV1	IntV2	ExtV1	ExtV2
SSB	GT 2	-11.3	-19.8	-14.0	-14.2	14.3	-9.2	9.6	9.9
	GT 3	-10.8	-16.5	-11.7	-11.8	9.4	-11.6	8.0	8.3
	GT 4	-10.3	-14.6	-9.6	-9.8	6.0	-12.0	6.9	7.0
	GT 5	-9.0	-13.4	-8.4	-8.3	4.6	-12.3	5.8	5.9
SIB	GT 2	-13.4	-22.0	-6.8	-9.4	-7.6	-23.2	-11.6	-9.9
	GT 3	-11.3	-18.5	-4.0	-6.5	-10.4	-21.8	-10.8	-9.3
	GT 4	-9.2	-15.8	-1.9	-5.5	-10.8	-19.8	-10.7	-8.7
	GT 5	-7.2	-13.1	-0.5	-4.8	-10.2	-17.0	-9.6	-8.2
AASHTO	GT 2	-14.1				40.5			
	GT 3	-17.2				31.9			
	GT 4	-20.3				26.2			
	GT 5	-22.7				23.0			

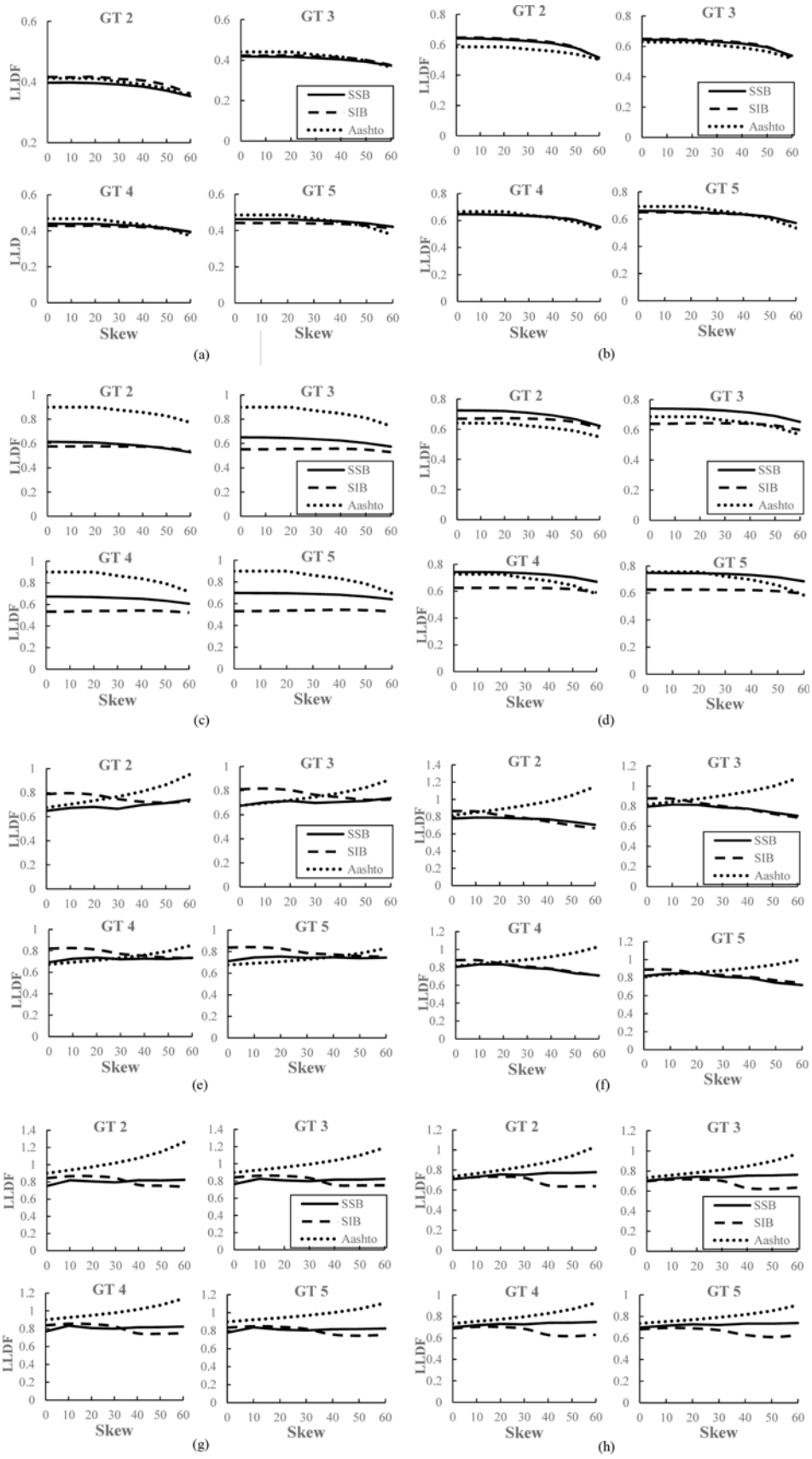

Fig. 4. Moment and Shear LLDFs vs. Skew Angles for Girder Types of (GT) of 2, 3, 4 and 5: (a) IntM1, (b) IntM2, (c) ExtM1, (d) ExtM2, (e) IntV1, (f) IntV2, (g) ExtV1, (h) ExtV2

Table 5. The Percentage Increase in LLDFs for Various Slab Thicknesses

		IntM1	IntM2	ExtM1	ExtM2	IntV1	IntV2	ExtV1	ExtV2
SSB	ts=0.15	-8.0	-12.9	-7.3	-7.8	4.5	-12.2	5.8	5.4
	ts=0.20	-10.3	-14.6	-9.6	-9.8	6.0	-12.0	6.9	7.0
	ts=0.25	-10.6	-16.4	-11.7	-11.8	9.7	-11.8	8.0	8.4
	ts=0.30	-11.0	-18.4	-13.3	-13.4	13.3	-10.6	9.1	9.5
SIB	ts=0.15	-6.8	-13.5	-1.3	-5.4	-10.2	-15.2	-9.0	-8.7
	ts=0.20	-9.2	-15.8	-1.9	-5.5	-10.8	-19.8	-10.7	-8.7
	ts=0.25	-11.1	-17.8	-2.8	-5.8	-12.4	-23.7	-13.7	-10.1
	ts=0.30	-12.8	-19.5	-4.1	-6.5	-13.0	-26.8	-18.1	-12.9
AASHTO	ts=0.15	-24.9				20.5			
	ts=0.20	-20.3				26.2			
	ts=0.25	-17.4				31.6			
	ts=0.30	-15.3				36.8			

increases, the effect of skew on LLDFs for both type of bridges ceases away. AASHTO SCFs (see Table 2) also include girder type by employing a parameter K_g in the equation. AASHTO SCFs for girder moment predict generally larger reduction in LLDFs as the skew increases compared to that of the SIBs. Furthermore, the effect of superstructure – abutment continuity on the distribution of girder live load moment is more significant for bridges with smaller skew and girder size.

Except for the interior girder shear for two or more lanes are loaded (IntV2) case, an increase in LLDFs for the girder shear of SSBs is observed for all girder types as the skew increases (see Table 4). This increase is more pronounced for smaller girder types. As previously mentioned, AASHTO specifies increasing shear LLDFs for both interior and exterior girders. However, for SIBs, shear LLDFs for all girder sizes and load cases decreases as the skew increases. This decrease is more pronounced for IntV2 case. Furthermore, the effect of girder type on shear SCFs for SIBs is significant only for the IntV2 case. Figs. 4(e)-(h) reveal that, the effect of superstructure-abutment continuity is more significant in the case of exterior girder shear LLDFs for bridges with larger skew. However, the same is true for the interior girder shear LLDFs for bridges with smaller skew.

Table 4 and Fig. 4 reveal that while AASHTO overestimates the shear SCFs, it underestimates the moment SCFs for SIBs.

The discussions above strengthen the need for the development of new SCFs for SIBs. In these new SCFs, the girder size parameter should be included in the developed equations for both girder shear and moment LLDFs.

7.4 Effect of Skew and Continuity versus Slab Thickness

The effects of skew and continuity on the distribution of girder live load moment and shear are illustrated in Fig. 5 for slab thicknesses of 0.15, 0.20, 0.25 and 0.30 m. In the figures, the LLDFs obtained for SSBs, SIBs and those calculated from the AASHTO formulae for the interior and exterior girders of slab-on-girder bridges are compared. Additionally, in Table 5 the percentage increases in the LLDFs, as the skew angle is increased from 0° to 60°, are given for interior and exterior girder moment and shear for various slab thicknesses (t_s).

For the girder moment, it is observed from the Figs. 5(a)-(d) and Table 5 that, LLDFs for ExtM1 of SIBs are almost constant as the skew increases. However, for other cases and for SSBs, the skew decreases the LLDFs. An increase in the slab thickness intensifies this diminishing effect of skew. Contrary to that, AASHTO produces smaller LLDFs, which is more pronounced for smaller thicknesses.

For girder shear LLDFs, the effect of superstructure – abutment continuity is clearly observed from Figs. 5(e)-(h) and Table 5. Skew results in smaller interior and exterior girder shear LLDFs for SIBs, whereas it produces larger LLDFs for SSBs except for the case of IntV2. It is also found that the effect of skew is more noticeable for both girder shear and moment of SSBs and SIBs with thicker slabs. AASHTO formulas produces overly conservative estimates for girder shear LLDFs for both type of bridges.

Figure 5 and Table 5 reveal that, slab thickness has insignificant effect on LLDFs of exterior girder moments (ExtM1 and ExtM2) and modest effect on the other LLDFs.

7.5 Effect of Skew and Continuity versus Number of Girders

The effects of skew and continuity on the distribution of girder live load moment and shear are illustrated in Fig. 6 *f*or various number of girders ranging between 4 and 7. In the figures, the LLDFs obtained for SSBs, SIBs and those calculated from the AASHTO formulae for the interior and exterior girders of slab-on-girder bridges are compared. In a recent study (Yalcin and Dicleli, 2013), it was shown that, shear and moment LLDFs for jointed bridges and shear LLDFs for integral bridges are insensitive to the change in the number of girders. This is also proven in Fig. 6 for 0° skew. Thus, both AASHTO LLDF and SCF equations do not include number of girders as a parameter.

Since moment LLDFs for IBs are sensitive to the number of girders, the recently proposed set of LLDF equations (Erhan and Dicleli, 2009) for integral bridges include the number of girders. The percentage increases in the LLDFs for interior and exterior girder moment and shear are given for various number of girders

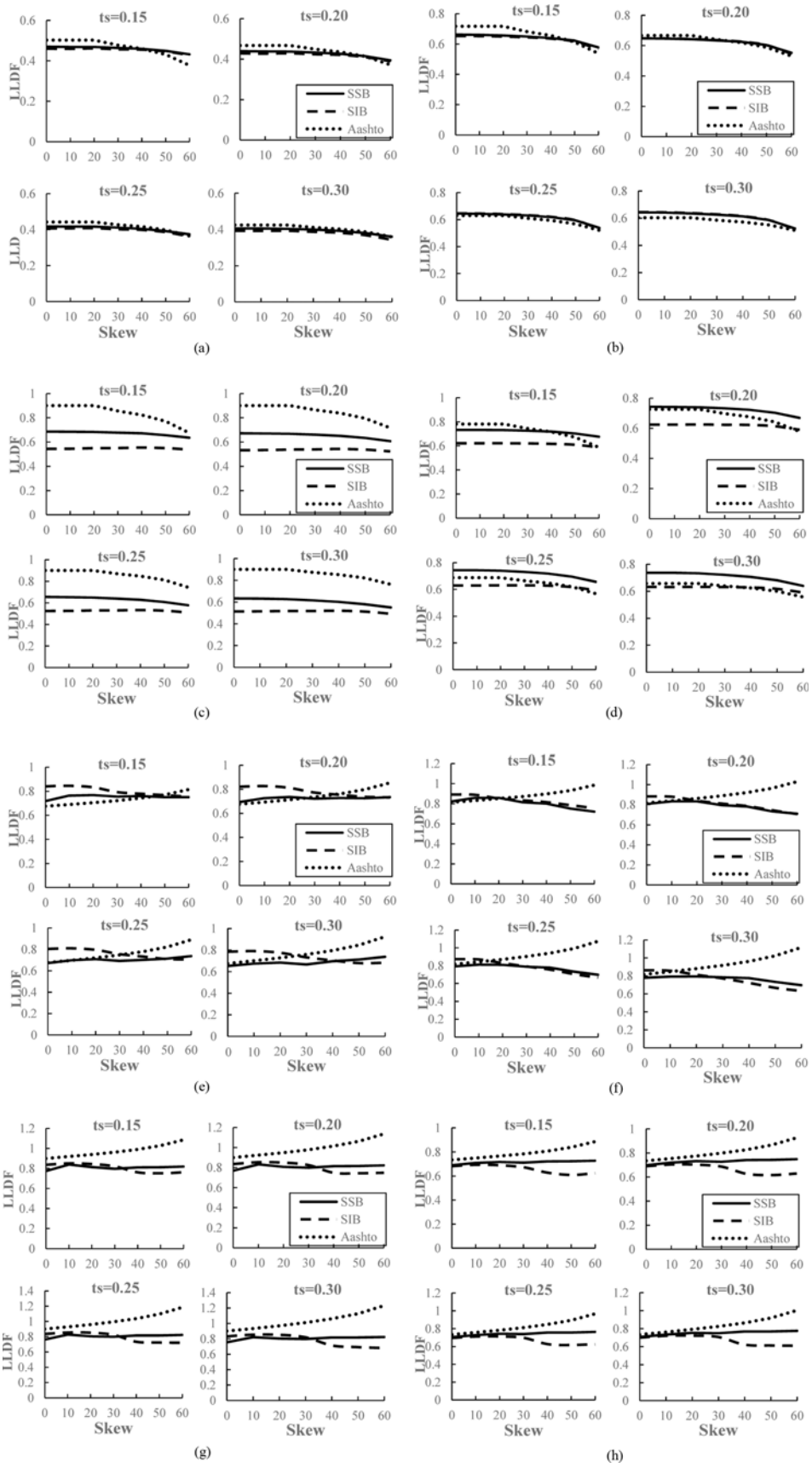

Fig. 5. Moment and Shear LLDFs vs. Skew Angles for Slab Thicknesses of (t_s) of 0.15 m, 0.20 m, 0.25 m and 0.30 m: (a) IntM1, (b) IntM2, (c) ExtM1, (d) ExtM2, (e) IntV1, (f) IntV2, (g) ExtV1, (h) ExtV2

Table 6. The Percentage Increase in LLDFs for Various Number of Girders

		IntM1	IntM2	ExtM1	ExtM2	IntV1	IntV2	ExtV1	ExtV2
SSB	Nb=4	-10.3	-14.6	-9.6	-9.8	6.0	-12.0	6.9	7.0
	Nb=5	-11.0	-16.9	-9.0	-10.1	6.6	-12.3	7.0	7.2
	Nb=6	-10.6	-16.6	-8.9	-9.9	6.7	-12.6	7.0	7.3
	Nb=7	-10.5	-16.5	-8.8	-9.9	6.8	-12.7	7.0	7.3
SIB	Nb=4	-9.2	-15.8	-1.9	-5.5	-10.8	-19.8	-10.7	-8.7
	Nb=5	-7.4	-15.6	-0.9	-3.0	-11.2	-20.0	-11.2	-9.4
	Nb=6	-6.2	-15.4	-0.2	-2.0	-11.6	-20.5	-11.8	-10.2
	Nb=7	-5.0	-14.1	0.5	-0.9	-11.8	-21.1	-12.3	-10.8
AASHTO	Nb=4,5,6,7	-20.3				26.2			

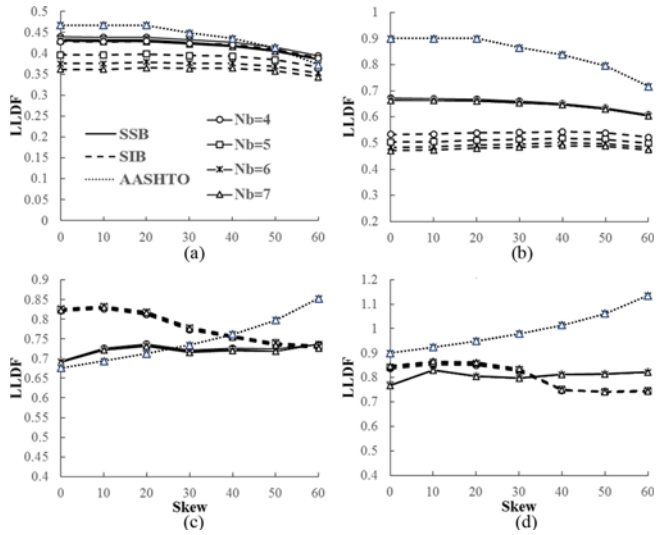

Fig. 6. Moment and Shear LLDFs vs. Skew Angles for Number of Girders of (Nb) of 4, 5, 6 and 7: (a) IntM1, (b) ExtM1, (c) IntV1, (d) ExtV1

(N_b) parameter in Table 6 for the case where the skew changes from 0° to 60°. It is observed from the table that AASHTO produces only one value for all the bridges having different number of girders.

In order to save space, Fig. 6 has only the results for the case where only one lane is loaded. Results for the case where two or more lanes are loaded are similar. As observed from the figure, only moment LLDFs for SIBs show some slight sensitivity to the number of girders parameter, while shear LLDFs remain insensitive. This is because shear effects remain localized on the bridge superstructure under live load. Therefore, in the studies directed towards the development of SCFs for SIBs, number of girder parameter should be included only for girder moment.

7.6 Effect of Skew and Continuity versus Girder Spacing

The effects of skew and continuity on the distribution of girder live load moment and shear are illustrated in Fig. 7 for girder spacings of 1.2, 2.4, 3.6 and 4.8 m. Additionally, in Table 7 as the skew changes from 0° to 60°, the percentage increases in the LLDFs for interior and exterior girder moment and shear are given for the Girder Spacing (*GS*) parameter. For the cases where two or more design lanes are loaded, the bridges having 1.2 m girder spacing can transversely accommodate only one design truck. Therefore, for these bridges, LLDFs for the case where two or more lanes are loaded, are not included in the figures and the table. On the contrary, the bridges with girder spacing of 4.8 m can transversely accommodate up to five trucks. It should be noted that AASHTO SCF equation for shear (see Table 2) does not include girder spacing parameter (*S*).

It is observed from Fig. 7 and Table 7 that skew has a decreasing effect on moment LLDFs of all bridges having various girder

Table 7. The Percentage Increase in LLDFs for Various Girder Spacing

		IntM1	IntM2	ExtM1	ExtM2	IntV1	IntV2	ExtV1	ExtV2
SSB	S=1.2	-5.1	-37.0	-7.7	-26.4	43.3	-25.2	13.4	-4.8
	S=2.4	-10.3	-14.6	-9.6	-9.8	6.0	-12.0	6.9	7.0
	S=3.6	-13.2	-20.6	-8.6	-11.1	-4.3	-12.6	-2.0	-1.1
	S=4.8	-12.8	-22.9	-7.2	-11.9	-1.1	-9.2	-3.6	-7.7
SIB	S=1.2	-4.8	-38.1	-4.0	-25.4	7.3	-31.8	-11.1	-30.7
	S=2.4	-9.2	-15.8	-1.9	-5.5	-10.8	-19.8	-10.7	-8.7
	S=3.6	-9.3	-18.2	-0.9	-4.9	-16.3	-27.0	-13.2	-12.9
	S=4.8	-8.6	-20.7	-0.3	-6.2	-9.8	-30.9	-8.1	-14.2
AASHTO	S=1.2	-14.4				26.2			
	S=2.4	-20.3							
	S=3.6	-24.9							
	S=4.8	-28.7							

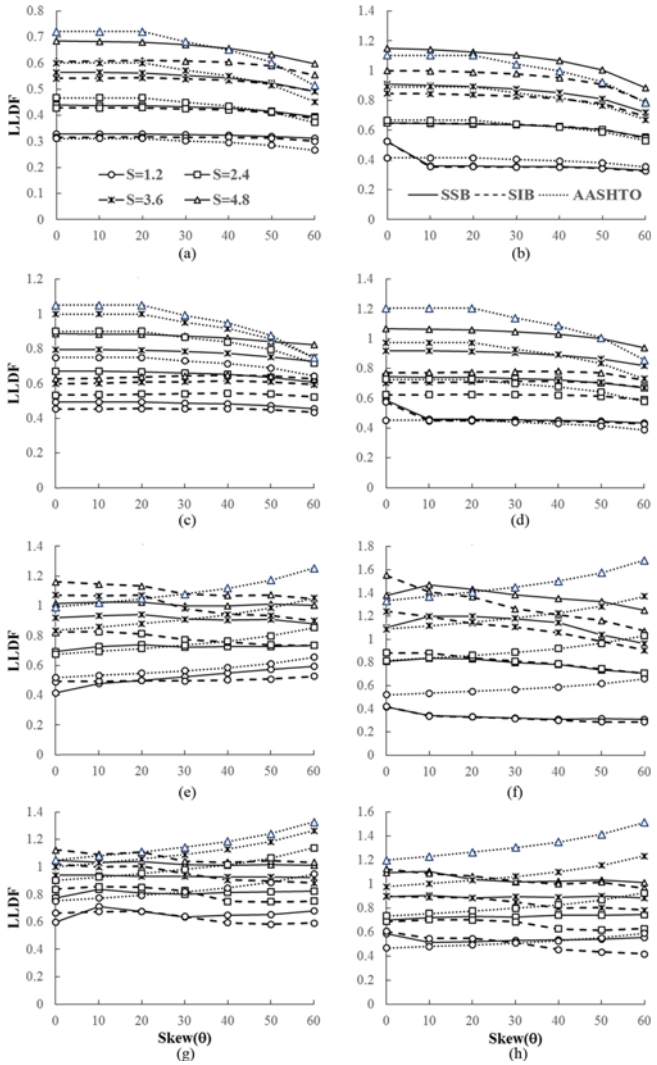

Fig. 7. Moment and Shear LLDFs vs. Skew Angles for Girder Spacings of (S) of 1.2 m, 2.4 m, 3.6 m and 4.8 m: (a) IntM1, (b) IntM2, (c) ExtM1, (d) ExtM2, (e) IntV1, (f) IntV2, (g) ExtV1, (h) ExtV2

spacing. This effect is more pronounced for IntM2 case. For girder shear, the effect of skew varies with girder spacing. For instance, as the skew increases, shear LLDFs of both SSBs and SIBs increase for S = 1.2 m, whereas the same LLDFs decrease for S = 3.6 m. As it can be observed from Table 7, AASHTO SCFs produces slightly conservative results for moment LLDFs and overly conservative estimates for shear LLDFs. Fig. 7 and Table 7 reveal that, although the effect of superstructure – abutment continuity on SCFs is prominent for girder shear, it is subtle for girder moment.

Furthermore, girder spacing has significant effects on both girder shear and moment LLDFs as observed from Fig. 7. Additionally, the figures demonstrate a poor distribution of live load effects among the girders of SIBs with larger girder spacing. Moreover, the difference between LLDFs of SSBs and SIBs becomes more significant as the girder spacing increases.

8. Conclusions

A parametric study is conducted to investigate the effects of superstructure-abutment continuity and skew angle on the distribution of live load shear and moment among the girders of SIBs. The SCFs obtained for SIBs are also compared with those calculated using AASHTO SCF equations to assess the applicability of AASHTO procedure to the design of SIBs. The conclusions are as follows.

1. The results reveal that, the superstructure-abutment continuity in SIBs improves the distribution of live load moment among the girders.
2. The effect of superstructure – abutment continuity causes a poor distribution of shear among the girders of SIBs for small skew angles and improved distribution for large skew angles.
3. Skew decreases the live load girder moment of both SIBs and SSBs and live load girder shear of SIBs. However, for SSBs skew has an increasing effect except for interior girder shear for two or more trucks loaded case.
4. AASHTO produces overly conservative estimates for shear SCFs and smaller estimates for moment SCFs for SIBs. Therefore, new SCF equations should be developed for SIBs.
5. Design engineers at the point of calculating LLDFs for SIBs using SCFs in AASHTO LRFD may utilize the findings of this study.
6. The effect of skew angle on girder moment LLDFs of SIBs is generally sensitive to all the superstructure parameters considered which are span length, girder type, slab thickness, number of girders and girder spacing. However, for girder shear LLDFs of SIBs, the effect of skew angle shows little or no sensitivity to the number of girders parameter.

Acknowledgements

The author would like to thank the Scientific and Technological Research Council of Turkey (TUBITAK) for the financial support provided to conduct this research study through project 114M006.

References

American Association of State Highway and Transportation Officials (AASHTO) (2014). *LRFD bridge design specifications 7th ed.*, American Association of State Highway and Transportation Officials, Washington, D.C.

Brockenbrough, R. L. (1986). "Distribution factors for curved I-girder bridges." *Journal of Structural Engineering*, Vol. 112, pp. 2200-15, DOI: 10.1061/(asce)0733-9445(1986)112:10(2200).

Burke, M .P. Jr. (2009). *Integral and Semi-Integral Bridges*, John Wiley and Sons: West Sussex, UK.

David, T. K., Forth, J. P., and Ye, J. (2014). "Superstructure behavior of a stub-type integral abutment bridge." *Journal of Bridge Engineering*, Vol. 19, 04014012, DOI: 10.1061/(ASCE)BE.1943-5592.0000583.

Dicleli, M. and Erhan, S. (2008). "Effect of soil and substructure properties on live load distribution in integral abutment bridges." *Journal of Bridge Engineering,* Vol. 13, pp. 527-539, DOI: 10.1061/(ASCE)1084-0702(2008)13:5(527).

Dicleli, M. and Erhan, S. (2009). "Live load distribution formulas for single-span prestressed concrete integral abutment bridge girders." *Journal of Bridge Engineering*, Vol. 14, pp. 472-486, DOI: 10.1061/(asce)be.1943-5592.0000007.

Dicleli, M. and Yalcin, O. F. (2014). "Critical truck loading pattern to maximize live load effects in skewed integral bridges." *Structural Engineering International,* Vol. 2, pp. 265-274, DOI: 10.2749/101686614x13830788506477.

Ebeido, T. and Kennedy, J. B. (1996). "Girder moments in simply supported skew composite bridges." *Canadian Journal of Civil Engineering,* Vol. 23, pp. 904-916, DOI: 10.1139/l96-897.

Erhan, S. and Dicleli, M. (2009). "Investigation of the applicability of AASHTO LRFD live load distribution equations for integral bridge substructures." *Advances in Structural Engineering*, Vol. 12, pp. 559-578, DOI: 10.1260/136943309789508500.

Erhan, S. and Dicleli, M. (2009). "Live load distribution equations for integral bridge substructures." *Engineering Structures,* Vol. 31, pp. 1250-1264, DOI: 10.1016/j.engstruct.2009.01.020.

Feldmann, M., Pak, D., Hechler, O., and Martin, P. O. (2011). "A methodology for modelling the integral abutment behaviour of non-symmetrically loaded bridges." *Structural Engineering International,* Vol. 21, pp. 311-319, DOI: 10.2749/101686611X13049248219962.

Franchin, P. and Pinto, P. E. (2014). "Performance-based seismic design of integral abutment bridges." *Bulletin of Earthquake Engineering,* Vol. 12, pp. 939-960, DOI: 10.1007/s10518-013-9552-2.

Hays, C. O., Sessions, L. M., and Berry, A. J. (1986). "Further studies on lateral load distribution using a finite element method." *Transportation Research Record*, Vol. 1072, pp. 6-14.

Imbsen, R. A. and Nutt, R. V. (1978). "Load distribution study on highway bridges using STRUDL finite element analysis capabilities." *Proceedings of conference on computing in civil engineering, ASCE,* New York.

Khaloo, A. R. and Mirzabozorg, H. (2003). "Load distribution factors in simply supported skew bridges." *Journal of Bridge Engineering,* Vol. 8, pp. 241-244, DOI: 10.1061/(ASCE)1084-0702(2003)8:4(241).

Mabsout, M. E., Tarhini, K. M., Frederick, G. R., and Tayar, C. (1997). "Finite element analysis of steel girder highway bridges." *Journal of Bridge Engineering,* Vol. 2, pp. 83-87, DOI: 10.1061/(asce)1084-0702(1997)2:3(83).

Nouri, G. and Ahmadi, Z. (2011). "Influence of skew angle on continuous composite girder bridge." *Journal of Bridge Engineering,* Vol. 17, pp. 617-623, DOI: 10.1061/(ASCE)BE.1943-5592.0000273.

SAP2000 Integrated Finite Element Analysis and Design of Structures Documentation (2014). Computers and Structures Inc., Berkeley, CA.

Tarhini, K. M. and Frederick, R. G. (1992). "Wheel load distribution in I-girder highway bridges." *Journal of Structural Engineering*, Vol. 118, pp. 1285-95, DOI: 10.1061/(asce)0733-9445(1992)118:5(1285).

Yalcin, O. F. (2015). "Truck loading positions for maximum live load girder moment in skewed integral bridges." In *International Conference of Computational Methods in Sciences and Engineering (ICCMSE 2015),* Vol. 1702. No. 1. AIP Publishing.

Yalcin, O. F. and Dicleli, M. (2013). "Comparative study on the effect of number of girders on live load distribution in integral abutment and simply supported bridge girders." *Advances in Structural Engineering,* Vol. 16, pp. 1011-1034, DOI: 10.1260/1369-4332.16.6.1011.

Yousif, Z. and Hindi, R. (2007). "AASHTO-LRFD live load distribution for beam-and-slab bridges: Limitations and applicability." *Journal of Bridge Engineering*, Vol. 12, pp. 765-773, DOI: 10.1061/(asce)1084-0702(2007)12:6(765).

Zokaie, T. (2000). "AASHTO-LRFD live load distribution specifications." *Journal of Bridge Engineering*, Vol. 5, pp. 131-138, DOI: 10.1061/(asce)1084-0702(2000)5:2(131).